Published in final edited form as:
Pigment Cell Melanoma Res. 2009 April ; 22(2): 187–195. doi:10.1111/j.1755-148X.2009.00544.x.

BI-69A11-mediated inhibition of AKT leads to effective regression of xenograft melanoma

Supriya Gaitonde[1], **Surya K De**[1], **Marianna Tcherpakov**[1], **Antimone Dewing**[1], **Hongbin Yuan**[1], **Megan Riel-Mehan**[1], **Stan Krajewski**[1], **Gavin Robertson**[2], **Maurizio Pellecchia**[1], and **Ze'ev Ronai**[1]

[1] Signal Transduction Program, Burnham Institute for Biomedical Research, 10901 N. Torrey Pines Rd. La Jolla, CA, USA

[2] Department of Pharmacology, The Pennsylvania State University, Hershey, PA, USA

Summary

The AKT/PKB pathway plays a central role in tumor development and progression and is often up-regulated in different tumor types, including melanomas. We have recently reported on the *in silico* approach to identify putative inhibitors for AKT/PKB. Of the reported hits, we selected BI-69A11, a compound which was shown to inhibit AKT activity in in vitro kinase assays. Analysis of BI-69A11 was performed in melanoma cells, a tumor type that commonly exhibits up-regulation of AKT. Treatment of the UACC903 human melanoma cells, har-boring the *PTEN* mutation, with BI-69A11 caused efficient inhibition of AKT S473 phosphorylation with concomitant inhibition of AKT phosphorylation of PRAS40. Treatment of melanoma cells with BI-69A11 also reduced AKT protein expression, which coincided with inhibition of AKT association with HSP-90. BI-69A11 treatment not only caused cell death of melanoma, but also prostate tumor cell lines. Notably, the effect of BI-69A11 on cell death was more pronounced in cells that express an active form of AKT. Significantly, intra-peritoneal injection of BI-69A11 caused effective regression of melanoma tumor xenografts, which coincided with elevated levels of cell death. These findings identify BI-69A11 as a potent inhibitor of AKT that is capable of eliciting effective regression of xenograft melanoma tumors.

Keywords

AKT; melanoma; BI-69A11; HSP90; Pten; PI3K

Introduction

The AKT signaling pathway is among the key tumor survival mechanisms. Three homologous AKT isoforms (AKT1, AKT2, and AKT3) are among the members of the AGC kinase family which are activated in response to survival signals. AKT activation is mediated by phosphatidylinositol 3-OH kinase (PI3K) which phosphorylates phosphatidylinositol-4,5-biphosphate (PIP2) to produce phosphatidylinositol-3,4,5-triphosphate (PIP3). PIP3, in turn, recruits AKT to the plasma membrane where AKT

CORRESPONDENCE Ze'ev Ronai, ronai@burnham.org.

Supporting information

Additional Supporting Information may be found in the online version of this article

Please note: Wiley-Blackwell are not responsible for the content or functionality of any supporting materials supplied by the authors. Any queries (other than missing material) should be directed to the corresponding author for the article.

Ser473 is phosphorylated by mammalian target of rapamycin (mTOR) or integrin linked kinase. Additional phosphorylation of Thr-308 at the catalytic site by the pyruvate dehydrogenase kinase isozyme 1 (PDK1) or the mTORC2 complex is needed for AKT activity. The PI3K contribution to AKT activation is counterbalanced by phosphatase and tensin homologue found on chromosome 10 (PTEN). Therefore, inactivation of PTEN, a common occurrence in human cancer, results in constitutively high level of AKT activity (Carracedo and Pandolfi, 2008; Yuan and Cantley, 2008).

Following its activation, AKT phosphorylates close to 100 substrates, through which it modulates a variety of cellular functions (Sheng et al., 2009; Cicenas, 2008; Yuan and Cantley, 2008). Those include AKT's ability to elicit an antiapoptotic effect through the phosphorylation and inhibition of key pro-apoptotic proteins, such as BAD, MDM2 and members of the Forkhead family; the support of cell proliferation by inactivating p27 and inhibition of glycogen synthase kinase 3 (GSK3)-mediated Myc and cyclin D1 inhibition; the effect on growth, metabolism and angiogenesis; and lastly, on protein translation and ribosome biogenesis. AKT increases translational machinery to produce ribosomes and increases the protein synthesis rate by dual regulation of the GTPase-activating protein (GAP) TSC2 and PRAS40 (a proline-rich AKT substrate of 40 KDa).

AKT activity, often measured by its phosphorylation at Ser473, has been linked to poor prognosis in several different cancers, including melanoma, acute myelogenous leukemia, lung, head and neck, breast, endometrial, brain, gastric, ovarian, colon and prostate cancer (Cicenas, 2008; Dai et al., 2005). The tumor promoting activities elicited by AKT have raised the notion that AKT may serve as an important target for cancer treatment (Garcia-Echeverria and Sellers, 2008). Accordingly, growing efforts are devoted to developing inhibitors to AKT. Of those developed so far, many were designed against the Pleckstrin Homology (PH) domain of AKT or the ATP-binding domain (Carnero et al., 2008; Lindsley et al., 2008).

AKT activation in melanoma is reported to occur in about 50% of cases, where only a portion of these (20–30%) are attributed to PTEN mutations (Goel et al., 2006; Haluska et al., 2006; Robertson, 2005). Activated AKT cooperates with the B-Raf, which is mutated in 70% of melanomas (Cheung et al., 2008). Consistent with its diverse tumor promoting functions, activated AKT enhances the conversion of the radial to vertical growth phase of melanoma, pointing to its role in progression and metastasis of melanoma (Fried and Arbiser, 2008; Govindarajan et al., 2007).

In this study we have characterized the AKT inhibitor BI-69A11 in UACC903 melanoma cells, which harbor a PTEN mutation, and in 29-1, a UACC903 variant that was reconstituted with chromosome 10 carrying a wt PTEN. We demonstrate the inhibition of AKT activity by BI-69A11 and its effect on melanoma cells in culture and xenograft models.

Results

Identification of BI-69A11 as AKT inhibitor

We recently reported on the direct evaluation of a number of *in silico* approaches to identify AKT inhibitors (Forino et al., 2005). We achieved experimental validation of selected compounds using both a fluorescence-based enzymatic assay and a substrate phosphorylation assay involving the protein GSK-3 (Forino et al., 2005). Briefly, the virtual docking approach consists of selecting the top 4000 out of 50 000 docked compounds, using a variety of computational docking approaches, including a consensus score among two different scoring functions (Forino et al., 2005). Of those, 100 compounds were selected

based on ranking and favorable docking geometry. Finally, compounds were selected for further evaluation based on their ability to inhibit AKT activity with IC_{50} values in the low micromolar range. Compound BI-69A11 (Figure 1) inhibited AKT1 in a concentration range comparable to that of H-89, a commercially available AKT inhibitor, yielding IC_{50} values of 2.3 μM, through an ATP competitive inhibition (Forino et al., 2005). BI-69A11 did not affect the activity of other protein kinases including Abl1, p38α, JNK, and PI3K, even at high concentrations of 100 μM.

Based on the docked geometry, and in agreement with our experimental data, it appears that BI-69A11 fits in the catalytic site of the ATP, resembling the binding of the adenosine moiety of the cofactor (Figure 1). The predicted binding mode of BI-69A11 in the ATP site of PKB/AKT (pdb: 1O6K) (Yang et al., 2002) suggests that it forms three hydrogen bonds with residues Lys181, Thr292, and Glu279 (Figure 1). These would account for its inhibitory properties against AKT and for the benzimidazole ring occupying an adjacent hydrophobic region. These favorable inhibitory properties of BI-69A11 promoted further synthesis and cell-based evaluations.

Characterization of BI-69A11 in melanoma cells

To evaluate the effectiveness of BI-69A11 on melanoma cells we assessed the effect of different concentrations on AKT phosphorylation in MeWo cells. While low doses (<0.3 μM) did not affect AKT phosphorylation, a dose of 3 μM BI-69A11 caused partial inhibition of AKT phosphorylation on S473, which serves as a marker for AKT activity (Figure 2A). Analysis of cell death revealed that about 60% of the melanoma cells were dead within 24 h after treatment with the 3 μM dose of BI-69A11 (Figure 2B). These data provide initial support for the effectiveness of this inhibitor on AKT phosphorylation and melanoma cell death.

To substantiate these initial findings we have set to compare the effect of the BI-69A11 on AKT phosphorylation and cell death among melanoma, prostate and breast tumor cell lines. Since the concentration of 3 μM caused partial inhibition of AKT phosphorylation, we have now compared the effect of two higher concentrations of BI-69A11, 5 and 10 μM. Compared with MeWO melanoma cells, PC3 prostate tumor cells were equally affected upon treatment with BI-69A11. In both cases, the basal level of AKT phosphorylation was effectively inhibited by the 5 μM, as well as the 10 μM dose (Figure 2C). Notably, the decrease in AKT phosphorylation at these doses of the BI-69A11 coincided with reduced levels of AKT protein (Figure 2C). In contrast, AKT protein levels were not affected in MCF7 cells, which do not express a constitutively active AKT (Lu et al., 2006; Figure 2B). These initial data suggest that AKT phosphorylation may be required for BI-69A11 to affect AKT, which causes a decrease in AKT protein levels, and which is also reflected at the level of its phosphorylation. Consistent with the effect of BI-69A11 on AKT phosphorylation was its effect on cell death. Within 4 h of treatment with 5 μM of BI-69A11 about 25% of both PC3 and MeWo cells underwent cell death (Figure 2D). Strikingly, such treatment did not affect viability of the MCF7 cells (Figure 2D). These data suggest that BI-69A11 causes effective death of tumor cells that express an active form of AKT. Consistent with these observations, melanocytes that are grown in culture in the presence of growth factors express active AKT; this is no longer seen if the cultures are deprived of these factors for 12–24 h. Growth factor-maintained melanocytes treated with BI-69A11 caused efficient inhibition of AKT phosphorylation, which coincided with cell death; whereas treatment of melanocytes deprived of growth factors (for 24 h) no longer elicit toxic effect (data not shown).

BI-69A11 inhibits AKT activity, AKT protein levels and AKT association with HSP-90

To further characterize the inhibition of AKT by BI-69A11 we used a set of melanoma cells in which PTEN is either inactive (UACC903 cells) or active because of reconstitution of chromosome 10 with wt PTEN (clone 29-1; Robertson et al., 1998).

The addition of BI-69A11 to UACC903 cells caused a dose-dependent decrease in the levels of pAKT Ser473 (Figure 3A). Thus, we set to test the possibility that BI-69A11's ability to inhibit AKT activity may stem from inhibition of AKT protein expression (Figure 3A total AKT levels). We thus assessed whether inhibition of AKT Ser473 phosphorylation coincides with its activity, namely the phosphorylation of known AKT substrates. As shown, phosphorylation of PRAS40 was markedly inhibited in these cells (Figure 3B). Of note, AKT3, the primarily active isoform of AKT in melanoma cells, effectively phosphorylates PRAS40 (Madhunapantula et al., 2007).

29-1 cells no longer express a constitutively active form of AKT (Robertson et al., 1998). To activate AKT, 29-1 cells were treated with IGF-1 (Figure 3B). While resulting in the activation of AKT and concomitant phosphorylation of PRAS40 (although to a lesser degree when compared with the UACC903 cells), the addition of BI-69A11 effectively inhibited the phosphorylation of PRAS40 (Figure 3B). These results suggest BI-69A11 may serve as a potent inhibitor of AKT activity.

Given the effect of BI-69A11 on the level of AKT protein, we assessed the possible mechanisms underlying such an effect. First, we assessed whether BI-69A11 affects the level of AKT transcripts. RNA prepared from the melanoma cells, with and without treatment with BI-69A11, was subjected to QPCR analysis. Such analysis did not identify differences in AKT transcripts (data not shown) suggesting that the inhibitor does not affect the mRNA levels of AKT.

Among cellular proteins implicated in the regulation of AKT levels is the cellular chaperone HSP-90. Inhibition of HSP-90's chaperone function, as commonly achieved by the geldanamycin antibiotic, interferes with the conformational maturation and refolding of its associated proteins, thereby promoting their degradation (Munster et al., 2002; Neckers and Neckers, 2002). AKT was shown to be affected either directly or indirectly by inhibition of HSP-90 (Basso et al., 2002; Fujita et al., 2002; Theodoraki et al., 2007; Xu et al., 2003). Thus, we assessed whether association of AKT with HSP-90 could be affected by BI-69A11. Immunoprecipitation of AKT from melanoma cells identified HSP-90 in the immunoprecipitated material. Such association was however abolished following treatment with the BI-69A11 inhibitor (Figure 3C). Since BI-69A11 causes reduced level of AKT protein (Figures 2C, 3A, 3C lysate panel) we monitored such association under conditions in which AKT levels are comparable. To this end, we have also performed the experiment in the presence of the proteasome inhibitor MG132. Although MG132 restored the level of AKT protein expression, it did not restore HSP-90-association with AKT (Figure 3C). These data suggest that the decrease in AKT levels seen following treatment with BI-69A11 can be attributed to disrupted association with the HSP-90 chaperone. To determine whether BI-69A11 may also affect other HSP-90 client proteins, we have monitored changes in the levels of p53 and c-Jun, two short-lived proteins that were shown to be among HSP-90 client proteins whose stability is affected by geldanamycin. BI-69A11 did not affect c-Jun protein levels, and had limited effect on the level of p53 (data not shown). These data imply that BI-69A11's effect on AKT interferes with its ability to associate with HSP-90.

BI-69A11 elicits more effective cell death in melanoma cells expressing active AKT

Since AKT activity is important for tumor cell survival, its inhibition is expected to result in cell death. We thus monitored cell death in melanoma cells that were treated with BI-69A11.

With concentrations as low as 1 μM, BI-69A11 caused effective cell death within 24 h following treatment. Interestingly, the effect of the inhibitor was more pronounced on PTEN mutant melanoma cells, compared with the 29-1 cells into which the wt PTEN was reconstituted (Figure 4A). Similarly, when compared with the earlier time point, BI-69A11 exhibited a stronger effect on the PTEN mutant melanomas, albeit a higher dose of the inhibitor was required to achieve cell death within the 6-h time point (Figure 4A). Consistent with these findings, PARP cleavage was more pronounced in the UAC903 cells, compared with the 29-1 line (Figure 4B). These data point to a more efficient effect of BI-69A11 on melanoma cells that harbor higher AKT activity.

BI-69A11 inhibits melanoma xenografts

In light of the efficient cell death elicited by BI-69A11, we assessed its activity on tumor growth in mouse xenografts. To this end, 903 human melanoma cells, which harbor a PTEN mutation, were injected subcutaneously into nude mice and tumors were allowed to form over a period of 10 days. When the tumors reached an approximate size of 1 mm^3, mice were injected intra-peritoneally twice per week with BI-69A11 (0.5–2.0 mg/kg), or with a control (dimethylsulfoxide (DMSO); 0.1%, used to dissolve the inhibitor). The selection of this dose-range for BI-69A11 was based on initial MTD assays, which revealed toxicity at the 5 mg/kg dose (data not shown). Strikingly, BI-69A11 effectively inhibits further growth of the melanoma tumors. Furthermore, treatment with the inhibitor caused efficient regression in these tumors (Figure 5A). Interestingly, lower concentrations of BI-69A11 were as efficient, and perhaps slightly more so, at inhibition of melanoma growth, compared with the higher ones (Figure 5A). An independent study using a range of 0.05–0.5 mg/kg confirmed that 0.5 mg/kg is the most effective dose (data not shown). Of note, removal of the inhibitor 3 days prior to termination of the experiment resulted in an initial increase in tumor size in mice that were treated with the low concentration of the inhibitor, but not in those that received the higher doses (compare 22 and 24 day bars in Figure 5A). Using TUNEL staining, analysis of the tumors from each of the treatment groups for apoptosis revealed higher degrees of apoptosis in the treatment groups compared with the control tumors. Strikingly, the tumors that were obtained from the lower-dose treatment exhibited higher levels of apoptosis (Figure 3B,C). These data suggest that BI-69A11-induced apoptosis is, in part, a mechanism by which it causes regression of the melanoma tumors tested here. The data also suggest that BI-69A11 elicits effective inhibition of melanoma tumor growth in vivo.

Discussion

The present study elucidates the activities of BI-69A11, a competitive inhibitor for AKT that was identified by using a virtual docking approach based on consensus scoring (Forino et al., 2005). Expected properties for this inhibitor, based on initial analysis, predicted competitive inhibition against AKT. Analysis of the inhibitor for its biological activities was made in melanoma cells in which AKT is commonly hyperactive. Using the 903 melanoma cell system we were able to compare the activities of BI-69A11 between the original cells where PTEN is deleted to those in which PTEN was reconstituted (clone 29-1). BI-69A11 was more effective in inhibiting AKT and eliciting cell death in the UACC903 cells that have higher levels of AKT activity. Of importance, the inhibitor was able to block IGF-induced AKT phosphorylation of PRAS40, a known downstream target of AKT, in the 29-1 cells, suggesting that it is capable of affecting physiological stimuli elicited in PTEN wt cells. BI-69A11 was as efficient in inhibition of AKT phosphorylation in other melanoma cell lines, including MeWO, as it was in the prostate tumor PC3 cells.

Importantly, BI-69A11's effect on AKT phosphorylation appears to be coupled with its effect on AKT protein levels. Our initial analysis reveals that AKT association with HSP-90

is inhibited in melanoma cells that were treated with BI-69A11. As inhibition of the HSP-90 complex with client proteins has been shown to affect their stability, this finding is likely to explain the nature of reduced AKT protein in BI-69A11-treated cells. Consistent with these observations, recent evidence indicates that mTORC2, a complex consisting of mTOR, SIN1, mLST8 and rictor, shown to phosphorylate AKT at Ser473, also causes stabilization of AKT through interaction with HSP-90, thus facilitating its protection through ubiquitin-mediated degradation (Facchinetti et al., 2008). We propose that dephosphorylation of AKT at this residue disables AKT-HSP-90 association, rendering AKT unstable. The latter is consistent with initial analyses of other HSP-90 client proteins whose stability is not affected by BI-69A11, compared with AKT.

Significantly, inhibition by BI-69A11 resulted in apoptosis of melanoma cells, consistent with previous reports of the effect of inhibiting AKT in such cells. Similarly, BI-69A11 caused efficient cell death in PC3 prostate tumor cells, which express active AKT. Of note, the degree of inhibition was greater in the tumor cells that harbor an active form of AKT, in agreement with the primary effect of this inhibitor on AKT activity. Consistent with these observations, the inhibitor did not affect the viability of MCF7 breast cancer cells, which do not express a constitutively active form of AKT, nor did it affect melanocytes that were deprived of growth factors, which would otherwise induce AKT activity. These findings substantiate the effectiveness of BI-69A11 on active AKT expressing cells. Significantly, BI-69A11 efficiently inhibited melanoma tumor growth and metastasis in a xenograft model. Overall, the present study provides initial characterization of an AKT inhibitor that affects select AKT signaling pathways. The effective cell death and inhibition of tumor growth in xenograft models justifies further studies of BI-69A11 for pre-clinical and clinical evaluations.

Materials and methods

Cell lines

UACC903 cells and 29-1 cells were cultured in Dulbecco's modified Eagle's medium (DMEM), supplemented with 10% fetal bovine serum (FBS) and maintained at 37°C in 5%CO_2.

Reagents and treatment protocol

Compound BI-69A11 was synthesized and purified as described herein. It was dissolved in DMSO and maintained as a 100 mM stock. Cells were plated to 75% confluency and grown overnight at 37°C. Plates were rinsed twice with a serum-free DMEM medium and the appropriate concentration of the compound was added to the plates. Cells were harvested at different timepoints by scraping (for western blotting) or trypsinization (for cell proliferation assay) where appropriate.

Chemistry

Unless otherwise indicated, all anhydrous solvents were commercially obtained and stored in Sure-seal bottles under nitrogen. All other reagents and solvents were purchased as the highest grade available and used without further purification. NMR spectra were recorded on Varian 300 or 500 MHz instruments. Chemical shifts (δ) are reported in parts per million (ppm) referenced to ^1H (Me_4Si at 0.00). Coupling constants (J) are reported in Hz throughout. Mass spectral data were acquired on an Esquire LC00066 for low resolution, a Micromass 70 SEQ for high resolution, or a JEOL LC-mate tuned for either low resolution or high resolution. The progress of reactions was monitored by TLC.

Synthesis of (E)-3-(3-(1H-benzo[d]imidazol-2-yl) acryloyl)-6-chloro-4-phenylquinolin-2(1H)-one (4, BI-69A11)

The compound was synthesized from (2-amino-5-chlorophenyl)-(phenyl)-methanone (compound 1 in Scheme S1, supporting information) through the Friedlander condensation reaction according to the reported procedures (De and Gibbs, 2005). To a solution of compound 3 (Scheme S1, supporting information) (511 mg, 1.72 mmol) in ethanol (8 ml), a 20% NaOH solution in water (1.3 ml) was added at room temperature. After stirring for 15 min, 1*H*-benzoimidazole-2-carboxaldehyde (376 mg, 2.58 mmol) was added to the reaction mixture and the resulting reaction mixture was stirred for 16 h at room temperature. Just before the completion of the reaction, it was neutralized with 1 N HCl, yielding a precipitate that was collected and purified by flash chromatography (60–80% ethyl acetate in hexane) to result in the final compound in 50% yield (330 mg).

Treatment with IGF-1

29-1 cells were plated at 75% confluency and grown overnight. The following day cells were rinsed twice with serum-free DMEM and the same containing 100 ng/ml IGF-1 was added to the cells. In cells treated with BI-69A11, 10 μM final concentration was added at the same time as IGF-1.

Western blotting

Cells were lysed in RIPA buffer containing 50 mM Tris–HCl pH7.4, 150 mM NaCl, 2 mM EDTA, 1% NP-40 (FLUKA Biochemika, Buchs, Switzerland), 0.1% SDS. The protein concentration was estimated using the Coomassie Protein assay kit (Thermo Scientific, Rockford, IL, USA). Equal concentrations of cell lysate (30–50 μg) were resolved on a 10% polyacrylamide gel and transferred onto Nitrocellulose membrane (GE Amersham, Uppsala, Sweden). Membranes were blocked for 1–2 h in either 3% bovine serum albumin (BSA) or 5% non-fat dried milk in Tris-buffered saline containing 0.05% Tween 20. Primary antibody incubations were performed overnight at 4°C with shaking. The blots were washed followed by incubation with a secondary antibody incubation for 1 h at room temperature. After washing, the blots were scanned on the Odyssey Licor scanner at the appropriate wavelength and the image was captured using the Odyssay software (LI-COR Biosciences, Lincoln, NE, USA).

Antibodies

pAKT473 was obtained from Cell Signaling Technologies (Beverly, MA, USA), total AKT, pPRAS40 and total PRAS40 from Biosource, PARP (Cell Signaling Technologies), c-Jun and p53 (Santa Cruz Biotechnology, Santa Cruz, CA, USA), HSP-90 (Abcam, Cambridge, MA, USA), and actin (Sigma, St. Louis, MO, USA). Secondary antibodies were goat anti-rabbit coupled to Alexafluor 580 and goat anti-mouse coupled to Alexafluor 800.

Proliferation assays

Cells were treated as described above. Instead of scraping cells into the serum-free medium, floating cells were collected in a 15 ml centrifuge tube whereas adherent cells trypsinized gently. The total cell population was pooled and counted on a hemocytometer after staining with Trypan Blue. The percentage of dead cells was determined by calculating the number of dead cells/total cells × 100. This experiment was performed two times each in triplicate.

Tumor studies

UACC903 cells (1×10^6) were injected subcutaneously and tumor size was monitored using calipers twice per week. Administration of BI-69A11 was performed twice weekly, via IP injection, when tumors reached an approximate size of $1mm^3$. Mice were injected with

different concentrations (0.5 mg/kg, 1.0 mg/kg, 2.0 mg/kg) of BI-69A11, or with control DMSO (0.1%) used to dissolve the inhibitor. All injections were put into a mixture of ethanol and cremophor (1:1) and suspended in saline (ethanol – cremophor 10% final concentration) for a total of 300 μl per injection. Intra-peritoneal injections were performed twice weekly, for a period of 3 weeks. At the end of the study, tumors were harvested, weighed and measured.

TUNEL assay and quantitative analysis

The detection of nuclei with fragmented DNA by terminal deoxyri-bonucleotidyl transferase–mediated dUTP nick end labeling (TUNEL) was accomplished using the ApopTag Peroxidase In situ Apoptosis Detection Kit (Chemicon, Temecula, CA, USA) according to the instructions of the manufacturer. Meyers Hematoxylin was used as a counterstain. Slides were scanned at 40× magnification (resolution of 0.25 μm/pixel [100 000 pix/in.]) using the Aperio ScanScope® CS system (Aperio Technologies, CA, USA). Spectrum Analytics package with nuclear algorithm and analysis software Image Scope (Aperio) were applied to quantify TUNEL positive cells present in the entire cross-sections of tumor specimens.

Computer modeling

The predicted binding mode of BI-69A11 in the ATP pocket of AKT (pdb:1O6K) was generated using the docking software GOLD (*GOLD*, version 3.2. The Cambridge Crystallographic Data Centre, Cambridge, UK).

Significance

Despite the fact that a large fraction of melanomas bear mutations in the MAPK signaling pathways, clinical trials using specific MEK and related MAPK inhibitors reveal equal effect on tumors that have, or not, such mutations. These observations, among others, point to the need to approach melanoma therapy with a combination of targeted therapy. One of the signaling pathways altered in melanoma is the PI3K/AKT signaling pathway. The present study provides initial characterization of an AKT inhibitor, BI-69A11, which inhibits AKT phosphorylation and expression levels. BI-69A11 effectively caused the death of melanoma cells in culture and the regression of melanoma xenografts, thereby justifying further studies for pre-clinical and clinical evaluations.

Supplementary Material

Refer to Web version on PubMed Central for supplementary material.

Acknowledgments

We thank members of the Ronai and Pellecchia laboratories and Marcia Dawson for help and advice. This study was supported in part by NCI grants CA111515 (to ZR) and CA052995 (to MP).

References

Basso AD, Solit DB, Chiosis G, Giri B, Tsichlis P, Rosen N. AKT forms an intracellular complex with heat shock protein 90 (Hsp90) and Cdc37 and is destabilized by inhibitors of Hsp90 function. J Biol Chem 2002;277:39858–66. [PubMed: 12176997]

Carnero A, Blanco-Aparicio C, Renner O, Link W, Leal JF. The PTEN/PI3K/AKT signalling pathway in cancer, therapeutic implications. Curr Cancer Drug Targets 2008;8:187–98. [PubMed: 18473732]

Carracedo A, Pandolfi PP. The PTEN-PI3K pathway: of feedbacks and cross-talks. Oncogene 2008;27:5527–41. [PubMed: 18794886]

Cheung M, Sharma A, Madhunapantula SV, Robertson GP. AKT3 and mutant V600E B-Raf cooperate to promote early melanoma development. Cancer Res 2008;68:3429–39. [PubMed: 18451171]

Cicenas J. The potential role of AKT phosphorylation in human cancers. Int J Biol Markers 2008;23:1–9. [PubMed: 18409144]

Dai DL, Martinka M, Li G. Prognostic significance of activated AKT expression in melanoma: a clinicopathologic study of 292 cases. J Clin Oncol 2005;23:1473–82. [PubMed: 15735123]

De SK, Gibbs RA. A mild and efficient one-step synthesis of quinolines. Tetrahedron Lett 2005;46:1647–49.

Facchinetti V, Ouyang W, Wei H, et al. The mammalian target of rapamycin complex 2 controls folding and stability of AKT and protein kinase C. EMBO J 2008;27:1932–43. [PubMed: 18566586]

Forino M, Jung D, Easton JB, Houghton PJ, Pellecchia M. Virtual docking approaches to protein kinase B inhibition. J Med Chem 2005;48:2278–81. [PubMed: 15801821]

Fried L, Arbiser JL. The reactive oxygen-driven tumor: relevance to melanoma. Pigment Cell Melanoma Res 2008;21:117–22. [PubMed: 18384505]

Fujita N, Sato S, Ishida A, Tsuruo T. Involvement of Hsp90 in signaling and stability of 3-phosphoinositide-dependent kinase-1. J Biol Chem 2002;277:10346–53. [PubMed: 11779851]

Garcia-Echeverria C, Sellers WR. Drug discovery approaches targeting the PI3K/Akt pathway in cancer. Oncogene 2008;27:5511–26. [PubMed: 18794885]

Goel VK, Lazar AJ, Warneke CL, Redston MS, Haluska FG. Examination of mutations in BRAF, NRAS, and PTEN in primary cutaneous melanoma. J Invest Dermatol 2006;126:154–60. [PubMed: 16417231]

Govindarajan B, Sligh JE, Vincent BJ, et al. Overexpression of AKT converts radial growth melanoma to vertical growth melanoma. J Clin Invest 2007;117:719–29. [PubMed: 17318262]

Haluska FG, Tsao H, Wu H, Haluska FS, Lazar A, Goel V. Genetic alterations in signaling pathways in melanoma. Clin Cancer Res 2006;12:2301s–2307s. [PubMed: 16609049]

Lindsley CW, Barnett SF, Layton ME, Bilodeau MT. The PI3K/AKT pathway: recent progress in the development of ATP-competitive and allosteric AKT kinase inhibitors. Curr Cancer Drug Targets 2008;8:7–18. [PubMed: 18288939]

Lu D, Huang J, Basu A. Protein kinase Cepsilon activates protein kinase B/Akt via DNA-PK to protect against tumor necrosis factor-alpha-induced cell death. J Biol Chem 2006;281:22799–807. [PubMed: 16785234]

Madhunapantula SV, Sharma A, Robertson GP. PRAS40 deregulates apoptosis in malignant melanoma. Cancer Res 2007;67:3626–36. [PubMed: 17440074]

Munster PN, Marchion DC, Basso AD, Rosen N. Degradation of HER2 by ansamycins induces growth arrest and apoptosis in cells with HER2 overexpression via a HER3, phosphatidylinositol 3′-kinase-AKT-dependent pathway. Cancer Res 2002;62:3132–7. [PubMed: 12036925]

Neckers L, Neckers K. Heat-shock protein 90 inhibitors as novel cancer chemotherapeutic agents. Expert Opin Emerg Drugs 2002;7:277–88. [PubMed: 15989551]

Robertson GP. Functional and therapeutic significance of AKT deregulation in malignant melanoma. Cancer Metastasis Rev 2005;24:273–85. [PubMed: 15986137]

Robertson GP, Furnari FB, Miele ME, Glendening MJ, Welch DR, Fountain JW, Lugo TG, Huang HJ, Cavenee WK. In vitro loss of heterozygosity targets the PTEN/MMAC1 gene in melanoma. Proc Natl Acad Sci USA 1998;95:9418–23. [PubMed: 9689095]

Sheng S, Qiao M, Pardee AB. Metastasis and AKT activation. J Cell Physiol 2009;218:451–4. [PubMed: 18988188]

Theodoraki MA, Kunijappu M, Sternberg DW, Caplan AJ. Akt shows variable sensitivity to an Hsp90 inhibitor depending on cell context. Exp Cell Res 2007;313:3851–8. [PubMed: 17643429]

Xu W, Yuan X, Jung YJ, Yang Y, Basso A, Rosen N, Chung EJ, Trepel J, Neckers L. The heat shock protein 90 inhibitor geldanamycin and the ErbB inhibitor ZD1839 promote rapid PP1 phosphatase-dependent inactivation of AKT in ErbB2 overexpressing breast cancer cells. Cancer Res 2003;63:7777–84. [PubMed: 14633703]

Yang J, Cron P, Good VM, Thompson V, Hemmings BA, Barford D. Crystal structure of an activated AKT/protein kinase B ternary complex with GSK3-peptide and AMP-PNP. Nat Struct Biol 2002;9:940–4. [PubMed: 12434148]

Yuan TL, Cantley LC. PI3K pathway alterations in cancer: variations on a theme. Oncogene 2008;27:5497–510. [PubMed: 18794884]

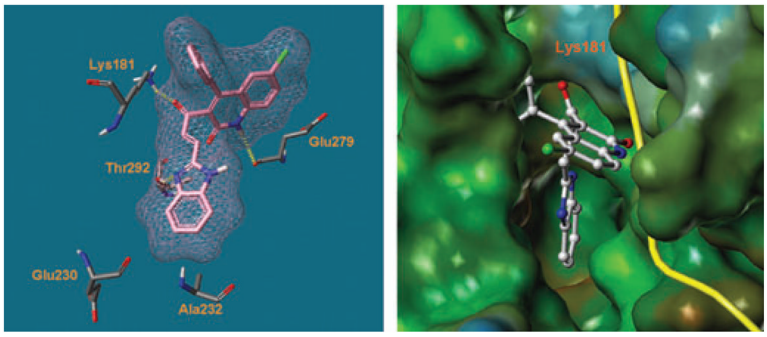

Figure 1.
Predicted binding mode of BI-69A11 in the ATP site of PKB/AKT. Hydrogen bonds are denoted by dashed cylinders in yellow.

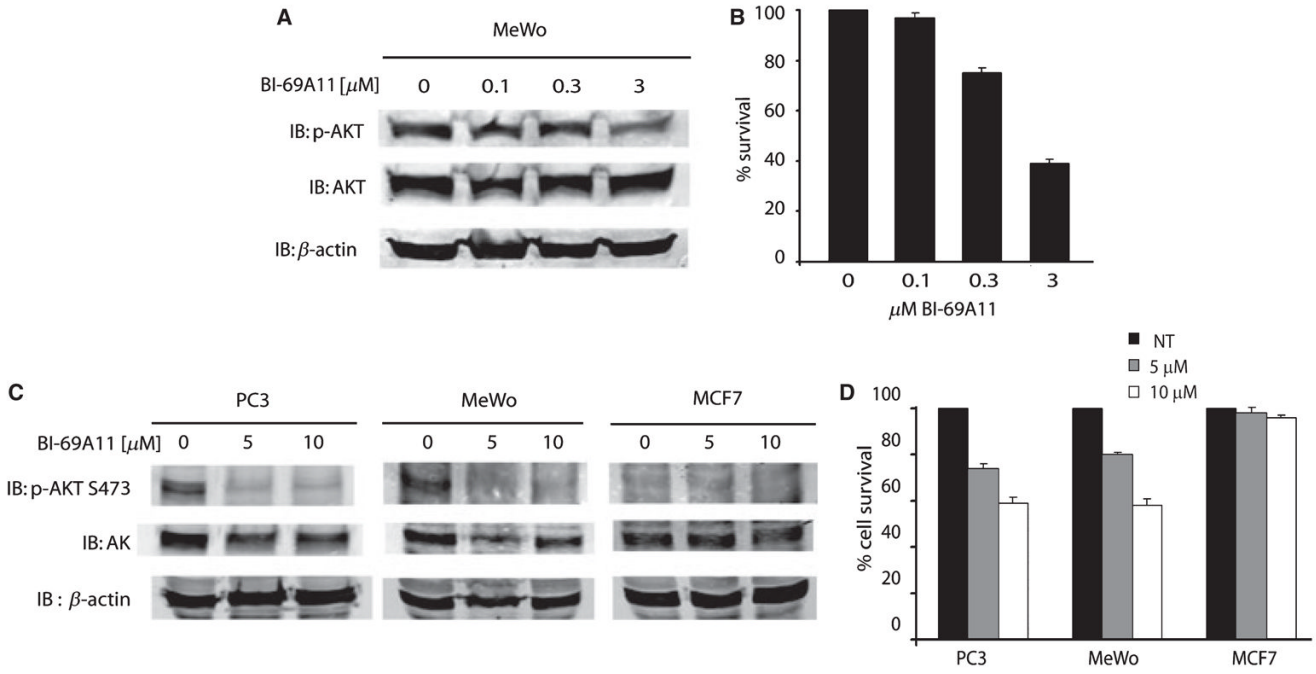

Figure 2.

Effect of BI-69A11 on melanoma and prostate cancer cells. (A) MeWo melanoma cells growing in 60 mm plates were treated with the indicated concentration of the inhibitor for 4 h before proteins were prepared for western blot analysis using the indicated antibodies. Level of β-actin was monitored as a control for protein loading. (B) Experiment was performed as indicated in panel A, except that cells were harvested after 24 h for analysis of cell survival using trypan blue staining. (C) Melanoma (MeWo), prostate cancer (PC3) and breast cancer (MCF7) cells were treated with BI-69A11 at the indicated concentrations; levels of AKT phosphorylation or expression were assessed 4 h later. The level of β-actin used as a control for protein loading. (D) Experiment was performed as indicated in panel C, except that cells were harvested after 4 h for analysis of cell death using trypan blue staining.

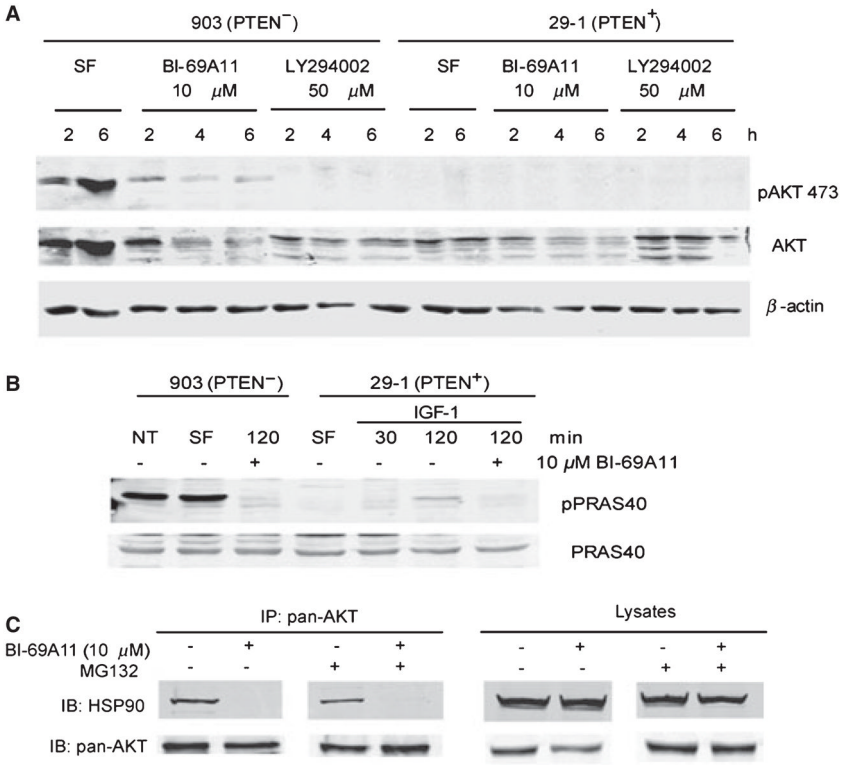

Figure 3.

BI-69A11 affects the phosphorylation and total levels of AKT in UACC903 (PTEN-) cells. (A) UACC903 and the modified clone 29-1 (PTEN+) cells were exposed to 10 μM BI-69A11 and 50 μM LY294002 (a PI3K inhibitor) and the levels of pAKT473 and total AKT determined by western analysis. Reduced levels of pAKT473 were observed in response to both BI-69A11 and LY, and reduced levels of total AKT were observed with increasing time after treatment with BI-69A11 in 903 and 29-1 cells. SF-serum-free. (B) BI-69A11 inhibits PRAS40 phosphorylation. UACC903 melanoma cells or 29-1 cells (PTEN+) were subjected to treatment with IGF-1 (20 ng/ml) and the level of PRAS40 phosphorylation was assessed. As indicated in Figure 3B, cells were also treated with BI-69A11 (10 μM). The cells were collected, lysed and levels of pPRAS40 and total PRAS40 determined by western analysis. (C) AKT association with HSP-90 is inhibited by BI-69A11. Human melanoma cells were treated with BI-69A11 (10 μM) or DMSO control for 4 h, followed by protein preparation and immunoprecipitation using antibodies to pan-AKT. MG132 treatment, when used, initiated 1 h prior to treatment and lasted up to the preparation of proteins (total of 5 h). The right panel depicts analysis of total lysates.

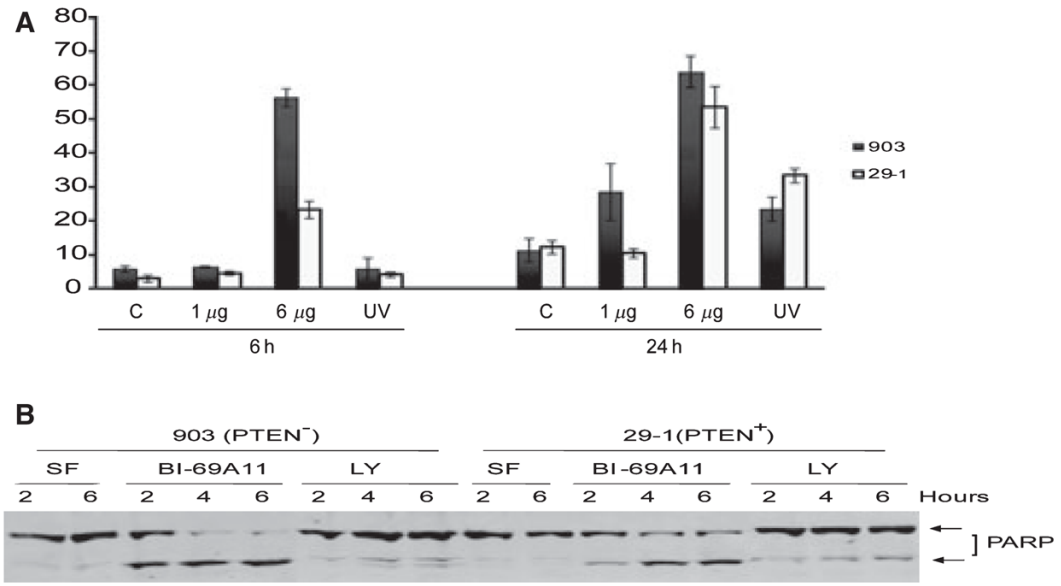

Figure 4.

BI-69A11 elicits more efficient cell death in UACC903 cells, compared with 29-1 cells. (A) 903 and 29-1 cells were exposed to different concentrations of BI-69A11 or UV light as a positive control and the percentage of cell death determined by trypan blue exclusion assay. (B) PARP cleavage was determined in 903 and 29-1 cells after treatment with BI-69A11 at 2, 4 and 6 h. Increased PARP cleavage is observed in 903 cells as compared to that observed in 29-1 cells after treatment with BI-69A11.

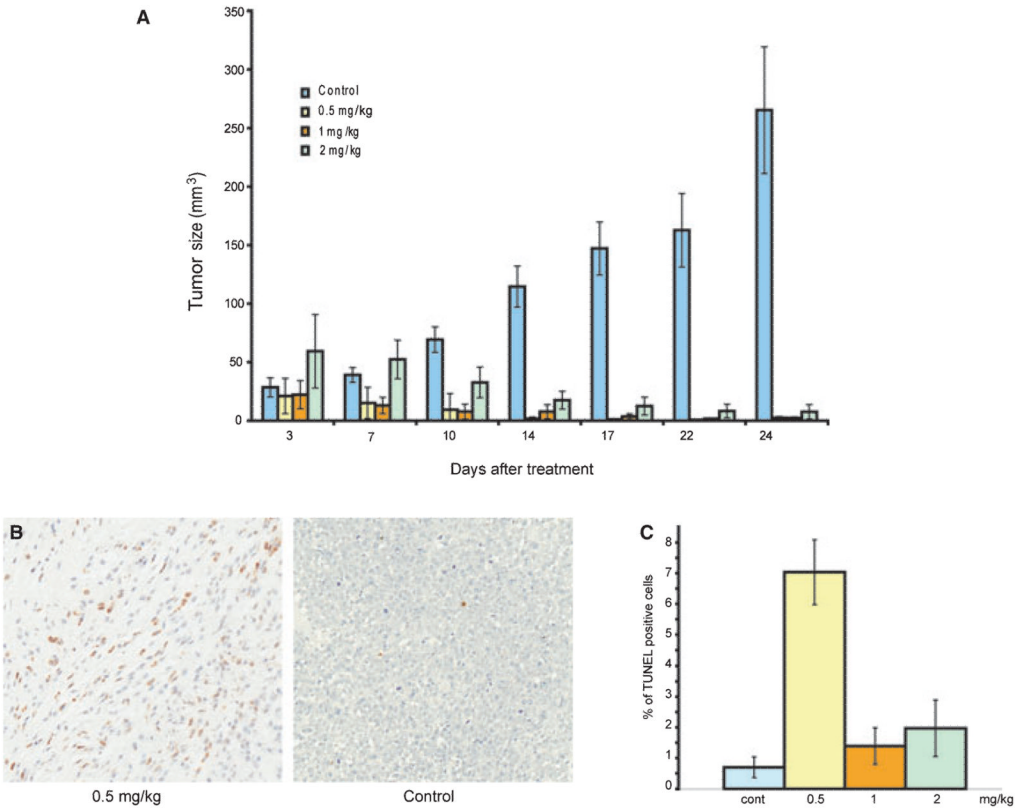

Figure 5.

BI-69A11 causes regression of melanoma tumors. (A) Nude mice were subcutaneously injected with UACC903 cells and tumors were allowed to reach an approximate size of 1 mm^3 before intra-peritoneal treatment was started; treatment was performed twice per week for 3 weeks with the indicated concentrations of BI-69A11. Each of the experimental groups consisted of 10 mice that were subjected to treatment with the indicated concentration of BI-69A11. Half of the animals were injected with tumor cells, and half with the control solution. Tumors were measured with calipers at the indicated time points. The mice were sacrificed and tumors harvested at the end of this period were measured and weighed to determine tumor volume and mass. Blue bars represent control-vehicle treated group; yellow bars represent the 0.5 mg/kg treatment group; the orange and green bars represent the 1 and 2 mg/kg treatment groups, respectively. (B) Analysis of cell death in the tumors was performed using TUNEL staining. Shown are representative pictures for control tumors (right) and a treatment group (0.5 mg/kg; left). (C) Quantification of TUNEL staining in the different tumor groups. Samples from each of the tumors were subjected to TUNEL staining which was quantified by Aperio ImageScope and confirmed by visual inspection of representative samples. The % of Tunel positive cells is indicated in the graph. Blue bars represent control-vehicle treated group; yellow bars represent the 5 mg/kg treatment group; the orange and green bars represent the 1 and 2 mg/kg treatment groups, respectively.